Aust. Met. Mag. 43 (1994) 219–228

Local-scale energy balances and microclimate in the desert ranges of central Australia

Helen A. Cleugh
School of Earth Sciences, Macquarie University, Australia
and
Tamsin Roberts
Areyonga School, Areyonga, Northern Territory, Australia

(Manuscript received July 1993; revised September 1994)

Direct observations of the surface energy balance and radiation budget are presented for a site within Australia's semi-arid interior ranges. These observations are interpreted in terms of those processes contributing to the local-scale climate. Measured albedo is lower (18 per cent) than those values often quoted for desert albedos, yielding high surface temperatures and soil heat flows. Extreme ranges in diurnal surface and air temperatures result from this high absorption of solar radiation and the low thermal diffusivity of the soil with concentrates heating into a shallow layer. This heated layer is rapidly depleted at night through large radiative losses that result from the extreme dryness of the atmosphere. No latent heat fluxes (positive or negative) were recorded. The lack of dew-fall is supported by the dew-point temperatures which were always less than air temperatures. All radiative energy is thus partitioned between convective and conductive sensible heating, with the magnitude of the ratio being determined by wind speed. These observations provide an insight into those microclimatic processes operating within the semi-arid landscapes of central Australia.

Introduction

One of the dominant controls on local-scale climates, together with the synoptic regime and geographic location, is the partitioning of the net all-wave radiative flux at the surface into various forms of heating. This surface energy balance, for heat transfer across an extensive, homogeneous surface plane, if advection and heat storage can be ignored, is written as:

$$Q^* = Q_E + Q_H + Q_G \qquad \ldots 1$$

where Q^* is the net all-wave radiation (this will either be a surplus or a deficit for a surface); Q_G is the sensible heat flow conducted into the substrate; Q_H is the convected sensible heat flow into the atmosphere and Q_E is the latent heat flux. By convention, positive heat fluxes refer to heat transfer directed away from the surface plane. The surface energy balance is often used as an explanatory tool in studies of the boundary-layer climates and meteorology of a location (e.g. Grimmond (1992), Grimmond et al. (1993) and Tapper (1988) all use the energy balance to explain and interpret those processes contributing to the climate above differing surface types).

There have been many overseas studies of boundary-layer processes and surface energy balances in semi-arid landscapes (e.g. southwest US: Kustas et al. (1991) and Grimmond (1991); Israel: Duvenani (1964), to name but a few). In contrast there have been surprisingly few studies of the semi-arid region of central Australia, despite the fact that 70 per cent of Australia's land area is characterised as 'semi-arid' (i.e. with an annual rainfall of less than 250 mm) and the influence that the desert regions of central Australia exert on the meteorology and climate of Australia (see discussion by Smith et al. (1994)).

The uniqueness of the 'Australian desert' is now being acknowledged (van Oosterzee 1991) and its similarity to the biophysical environments of deserts in other continents cannot be assumed. As more is learnt about the ecology of central Aus-

Corresponding author address: Dr H.A. Cleugh, Centre for Environmental Mechanics, CSIRO, PO Box 821, Canberra, ACT 2601, Australia.

tralia's deserts, particularly their flora and fauna, there will be a need to better understand the microclimate. The role of dew-fall in plant growth is an example of a potentially important aspect of the microclimate in central Australia. Dew-fall amounts are typically assumed to be negligible, yet personal observations (Roberts, personal communication) suggest that dew may comprise a significant component of a plant's water balance, especially during winter in the valleys sited within the ranges surrounding the Alice Springs area. Overseas studies have quantified dew-fall amounts but, recalling van Oosterzee, such results should not be uncritically applied to Australia.

A quantitative knowledge of the climate, especially climate parameters such as albedo and roughness, is also essential for numerical models of the global and regional climate. Current models representing central Australia use desert input parameters that are often derived from studies elsewhere, satellite 'observations' or are simply best guesses. For example, the plethora of modelling studies in the late 1970s investigating the feedback between albedo, rainfall and desertification all used albedos derived from northern hemisphere or western African deserts (e.g. Charney et al. 1977). Regional and global-scale climate scenarios for Australia depend on an accurate parametrisation of the land surface, hence the input of correct surface parameters for central Australia is crucial.

Probably one of the most extensive datasets for central Australia was obtained at Daly Waters, during the Koorin experiment. These measurements represent savanna land-use (eucalypt trees and native grasses) at a latitude of 15°S where the synoptic regime is dominated by the seasonal shift in the ITCZ and the wet season. There have only been a few other microclimate studies in semi-arid regions of Australia. Kalma and Badham (1972) measured radiation fluxes over bare soil and tropical pasture at Katherine (14°S 132°E). Detailed studies of radiation and heat fluxes over various salt lake systems in New South Wales have been conducted by Tapper (1988, 1991) and in South Australia by Hacker (1988) in order to understand mescoscale thermal circulation systems. More recently, as a part of the Central Australian Fronts Experiment (CAFE), energy balance measurements were conducted over natural grassland during September at 'Hughenden' (21°S, 144°E) in northern Queensland (Smith et al. 1994). The current bunny fence experiment (Lyons et al. 1993) will provide similarly useful information for the semi-arid landscapes bordering South and Western Australia. These studies provide some understanding of climatic processes for a few of the land surfaces and synoptic regimes present in Australia's semi-arid regions. Only the studies of Smith et al. (1994) and Kalma and Badham (1972) represent the dry, subtropical landscapes characteristic of central Australia.

This paper presents observations of the surface energy balance, radiation budget and local-scale climate at a site within the semi-arid, desert landscapes of central Australia which were measured in support of a longer term study of dew-fall occurrence. This microclimate study is entirely preliminary and exploratory, with the specific objective of understanding those mechanisms that determine the local-scale climate by observing both the climate and the radiation and energy partitioning. Although these are only short-term measurements at a single site, which is far from ideal, they provide some of the few direct measurements of energy and radiation balance components in these desert ranges and as such they contribute to an understanding of the climate processes in this unique environment. While the site cannot be said to represent the regional landscape (which has considerable heterogeneity induced by topography), these observations provide an insight into the surface energy exchange and microclimate over a surface which represents one element of this regional landscape. Furthermore, access to much of this area can only be gained by permission from the Aboriginal landowners and thus it is unlikely that many groups would be given the freedom of access offered to the authors. We thus present these data and analyses in the spirit that they offer a unique dataset and insight that would otherwise be all but impossible to obtain. To this end, the authors are unaware of any similar such observations in similar geographical regions.

Methods and site description

Microclimate station

To obtain the local-scale observations, a microclimate measurement station was established within, and to one side of, a broad, east/west oriented valley 5 km to the west of the community of Areyonga, Northern Territory, Australia (24°S 132°E, Fig. 1(a)). Areyonga, elevation ca. 500 m, is located 150 km west of Alice Springs and to the south of the Macdonnell Ranges. The valleys surrounding Areyonga are a part of the James Range and the local streams drain into the Palmer River. For security and other logistic reasons it was necessary to position the measurement station within an ephemeral creek bed which forms a small valley running perpendicular (i.e. north/south) to the main valley. The entire valley was sparsely vegetated, dominated by mulga (mostly *acacia aneura*, up to 3 m tall) and occasional river gums. The bushes surrounding the site included a native orange tree (*capparis mitchelli*, 2 m tall) and a caper bush (*capparis spinosa*). The density of spacing of vegetation in the main valley is estimated as ca. 20 per cent, with typical spacing of ca. 30 m. Using van Oosterzee's (1991) classifi-

Fig. 1 (a) Location map of central Australia and Areyonga. (b) Sketch map of measurement site.

(a)

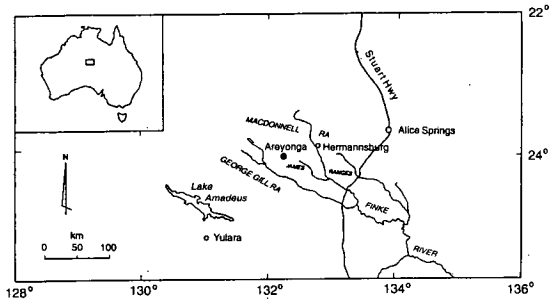

(b)

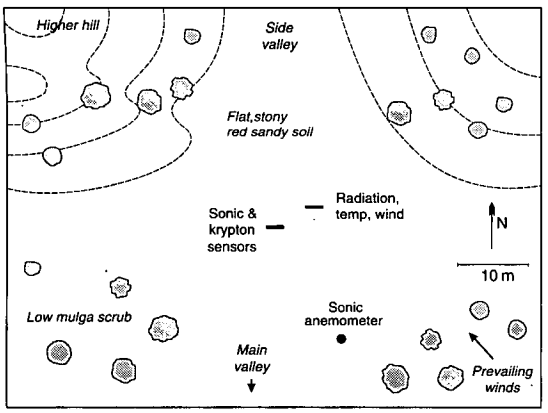

cation, the landscape is representative of the desert ranges and mulga woodlands ecosystems.

The microclimate measurement station is thus far from the uniform, flat site with extensive fetch that is considered to be necessary for accurate measurements of turbulent fluxes. Most of the diurnal air-flow was from the southerly sector (SE/SW) viz. from the main valley floor towards the valley side and hence the measurement station (Fig. 1(b)). Anabatic (by day) and katabatic (by night) flows up/down the low hillside 50 m behind the site may affect the flux measurements. Furthermore, fluxes were measured below the vegetation canopy height (see below for further detail). Although this canopy was very sparse, there is unlikely to be a fully adjusted, constant flux-layer and so the turbulent flux measurements may be in error. Because of these site limitations, careful checking for data consistency is an essential component of the study, including a check on mean vertical wind speeds, energy balance closure and spatial representativeness of surface fluxes.

Measurements

Continuous measurements were conducted from 21 July (YD 92/203) to 1 August (YD 92/213) 1992. The synoptic situation over central Australia during this period yielded persistent east to southeast trade wind-flow. A shift occurred from strong SE flow from 21–25 July to lighter NE–N flow in the latter part of July and early August. The climate over the area in July was marked by 'near extreme' (Bureau of Meteorology 1992) low relative humidities and high sunshine hours. Lowest temperatures occurred on 21 July and 10–12 July. The highest temperatures were recorded on 28 July.

Direct measurements were obtained of all energy balance components and enough of the radiation fluxes to enable computation of the full radiation budget. A Campbell Scientific (CSI) one-dimensional sonic anemometer with a fine wire thermocouple (12.7 μm) sensed the vertical wind speed (w′) and air temperature (T′) fluctuations while a krypton hygrometer (CSI, Model KH20) sensed the humidity (q′) fluctuations. These signals were sampled at 10 Hz and recorded on a CSI 21X micrologger which computed 15-minute averages plus variances, covariances (w′T′; w′q′) and correlations. The covariances were used to compute the sensible and latent heat fluxes (Q_H and Q_E). These two eddy correlation sensors were deployed adjacent to each other at a height of 1.5 m.

Two soil heat flux sensors were used: one buried at 0.07 m ($=Q_{G2}$) and another immediately beneath the surface at 0.01 m ($=Q_{G1}$). A CSI averaging thermocouple system (comprising two thermocouple probes) was positioned at 0.04 m to enable the heat storage between Q_{G2} and the surface to be computed, and thus Q_G at the surface ($=Q_{G0}$). Values for the volumetric heat capacity of sand were simply obtained from published values (Oke 1987). As Fig. 2 shows, Q_{G0} and Q_{G1} were in good agreement.

An unpurged net pyrradiometer (REBS, Model Q-6) was used to measure all-wave net radition (Q^*). Incoming and reflected short wave radiation ($K\downarrow$ and $K\uparrow$) were measured with a Middleton net pyranometer, where the outputs were separated to yield the downward and reflected components. Both radiation sensors were mounted at a height of 1 m and were calibrated prior to the study against a field standard. Differences were less than five per cent. An Everest 60° FOV infrared radiometer was positioned at 1.6 m, pointing towards the ground at a zenith angle of 45° and oriented south. The measured surface temperature allowed the computation of the upwelling long wave radiation flux ($L\uparrow$). The Everest sensor had not been recently calibrated so was checked against a calibrated hand-held infrared radiometer twice daily in the field. These two measures of surface temperature agreed to within 1°C. The downward long wave radiation ($L\downarrow$) can thus be computed as the residual in the radiation budget, although this will accumulate all measurement errors into $L\downarrow$ (see below for error analysis).

Fig. 2 Comparison of near-surface hourly soil heat fluxes computed (Q_{G0}) and measured (Q_{G1}).

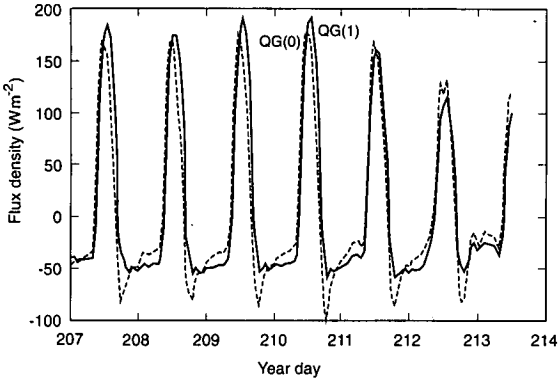

Relative humidity (RH) and air temperature (T) were sensed using a Rotronics sensor mounted in an unaspirated radiation shield at 1.4 m. An R.M. Young cup anemometer and wind vane, mounted at 1.3 m (cup height), yielded wind speeds and direction. The anemometer was calibrated in a wind tunnel 15 months prior to the study, and had only been used briefly since the calibration. The RH/T sensor was compared twice daily during the study using an aspirated Assman psychrometer. Air temperatures agreed to within 0.5°C (close to the limits for reading the scale on the Assman psychrometer). Over the range in RH (20–60 per cent) maximum differences of six per cent were found (the Rotronics sensor consistently showed higher values of RH). If the Rotronics sensor values are taken as incorrect, such discrepancies would lead to errors in vapour pressure (e) of six per cent of the saturation vapour pressure, viz, from 1–2.1 hPa over the range of temperatures recorded. This translates to an error of +/− 1°C in dew-point temperature (T_{dew}).

Independent measurements of all the components in (Eqn 1) will lead to an energy balance which does not close, i.e.:

$$Q^* = Q_H + Q_E + Q_G + \delta r \qquad \ldots 2$$

where δr is termed the residual and may be positive or negative, δr arises through the accumulation of measurement errors for each of the terms in (Eqn 1), or because some of the underlying assumptions are not met. The most likely cause of the latter is advection (horizontal heat transfer) or heat storage. A heat storage term must be included if the energy balance is defined for a volume, rather than heat transfer across a plane.

Error analysis

Based on manufacturer's specifications or instrument calibrations and intercomparisons, measurement errors typical of each sensor are: net radiation, five per cent; solar and reflected radiation, five per cent; surface temperature, 1.0°C; emitted long wave radiation (as a result of surface temperature errors), one per cent; T_{air} and T_{dew}, +/− 0.5 and 1°C respectively; wind speed, five per cent.

Errors in sensible heat flux measurements arise from errors in the sonic anemometer and thermocouple sensors plus any errors arising from incorrect application of the eddy correlation technique (e.g. non-zero vertical velocities). The former source of error is estimated to be less than ten per cent (Tanner, personal communication). Intercomparisons between the system and other eddy correlation sensors and methods of determining turbulent heat fluxes (e.g. Bowen ratio methods) show flux differences less than 15 per cent (e.g. Cleugh and Oke 1986) for both Q_H and Q_E which indicates the accuracy of these eddy correlation systems.

Errors in L↓ result from the accumulation of errors from the individual radiation sensors. It cannot be assumed that these are additive, although a simple linear sum of the component errors would represent the most conservative error estimate (Kalanda et al. 1980; Cleugh and Oke 1986). For L↓ this translates into errors of ca. 16 per cent of Q* for | Q* | greater than 50 Wm^{-2}.

Results and discussion

Radiation balance

The time series for all the radiation components, including Q*, is shown in Fig. 3(a) and the daytime and daily average fluxes are in Table 1.

For daytime measurements (Q*>0) the albedo averaged 17.44 per cent, ranging from 16.9–17.8 per cent. This is considerably lower than might be

Table 1. Average radiation and climate data.

$K\downarrow$ (Wm^{-2})	$K\uparrow$ (Wm^{-2})	$L\downarrow$ (Wm^{-2})	$L\uparrow$ (Wm^{-2})	T_s (°C)	T_{air} (°C)	RH (%)	T_{dew} (°C)
(a) Daily (24 Hour) averages (except short wave fluxes)							
500	87.2	281	393	15.4	13.5	31.6	−4.3
(b) Daytime (Q*>0) averages							
500	87.2	311	463	27.5	20.8	24.3	−3.6

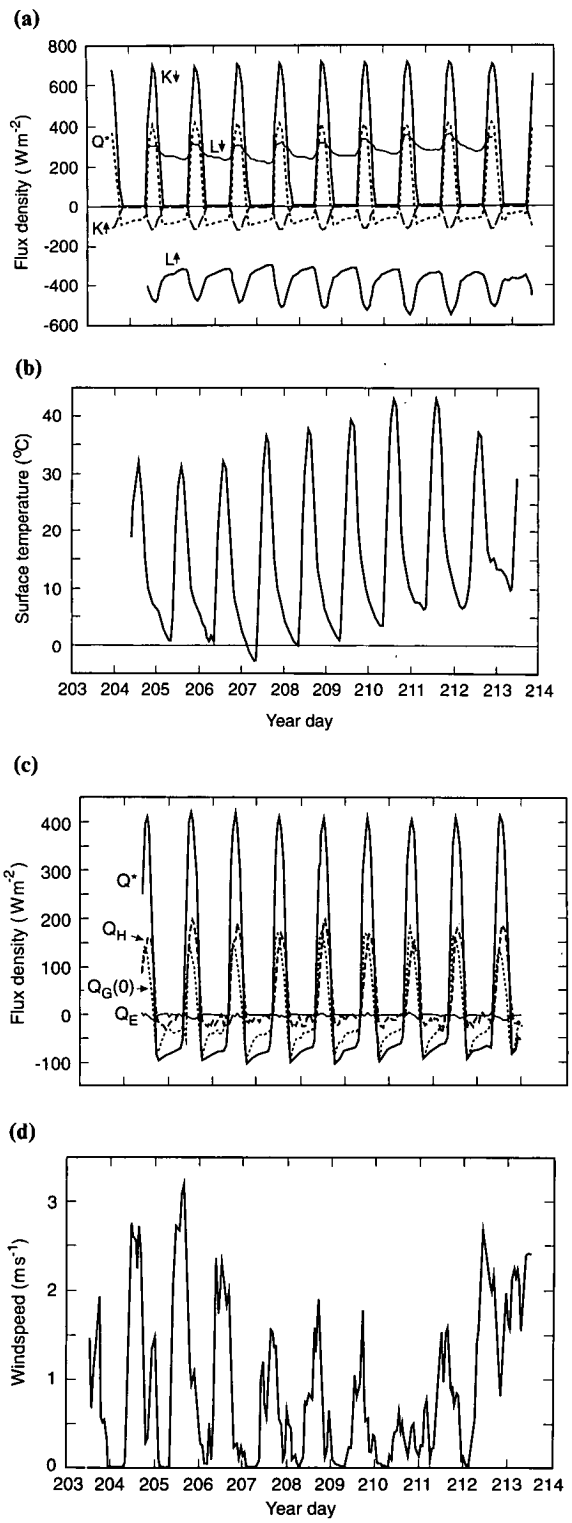

Fig. 3 Time series of hourly: (a) radiation fluxes; (b) surface temperatures; (c) net all-wave radiation, sensible, soil and latent heat fluxes; (d) wind speeds.

expected for soils in a 'desert' environment. The Koorin dataset does not include albedo, but Hyde (personal communication) found an albedo of 30 per cent for red sand and 50 per cent for white sand at Lake Mungo, NSW (30°S). Measurements conducted over native mallee vegetation in Hincks Park, South Australia, found a lower albedo of 12 per cent (Huang et al. 1993). This lower albedo illustrates the radiative trapping role of vegetation in a plant canopy. The albedo measured at this site is for bare soil only. The only other values for similar latitudes and land use are those from Kalma and Badham (1972), where an albedo of 25 per cent was found for bare soil. Interestingly, the satellite measurements conducted during the Earth Radiation Budget Experiment (ERBE) yield an albedo of ca. 18 per cent for this area, compared to 40 per cent for the Saharan and Saudi Arabian deserts and 25–30 per cent for the Gibson and Gobi deserts (Ramanathan et al. 1988). The combination of red soil plus the rocky texture of the ground surface enhances the trapping capability of the surface. We can thus expect that surface and soil temperatures will be large, as will soil heat fluxes. The ratio of net all-wave to incoming short wave radiation was 0.54, closely matching most approximate 'rules of thumb' and providing a check on the validity of the measurements.

The dominant feature of the radiation variation is the day-to-day consistency in the short wave forcing, with less than five per cent variation over the 10 measurement days. This reflects the constant nature of the atmospheric transmissivity, i.e. atmospheric aerosol concentrations and water vapour concentrations, characteristic of these latitudes in July. Reflected short and net all-wave radiation show similarly little variation. Thus the increase in L↑ resulting from the increase in surface temperature (Fig. 3(b)) is matched by an increase in L↓. Of course, these values for L↓ are derived as residuals and thus contain all the measurement errors from the other components, they are probably accurate to around 16 per cent of Q* as detailed above. This increase in calculated L↓ is consistent with the trend of increasing air temperature and humidity, thus offering some confirmation of the validity of the L↓ values. They are smaller than those measured under similarly dry skies in Niger, West Africa (Culf and Gash 1993), which ranged from 350 to 400 Wm^{-2}, but these differences are typical of the differences found between measurements conducted in the northern and southern hemispheres.

Some further indication of the validity of these fluxes is realised by comparison with values modelled using two popular formulae: Idso and Jackson (1969) (IJ) and Brunt (1932). These formulae are included in Table 2. The residual estimates of L↓ are smaller and larger than those modelled using the IJ and Brunt equations,

Table 2. Comparison between hourly estimates of downwelling long wave radiation.

Method	*Formulae for clear sky emissivity and L↓*	*Mean L↓ (Wm^{-2})*	*Mean absolute error (Wm^{-2})*	*Root mean square error (Wm^{-2})*
Brunt (1932)	$\varepsilon(0) = 0.61 + 0.05\sqrt{e_a}$; $L\downarrow = \varepsilon(0)\,\sigma T_a^4$	277.9	16.5	20.2
Idso and Jackson (1969)	$\varepsilon(0) = 1\text{-}0.261 \exp\{-7.77 \times 10^{-4}(273-T_a)^2\}$; $L\downarrow = \varepsilon(0)\,\sigma T_a^4$	302.9	24	30.8
Measured (by residual)	$L\downarrow = Q^* - K^* + L\uparrow$	285.8		

respectively. The summary statistics provided in Table 2 show that L↓ modelled using Brunt's equation shows slightly better agreement with L↓ estimated as a residual. Culf and Gash (1993) also noted that those models with both temperature and vapour pressure functions performed best. The differences between modelled and residual values are smaller than the measurement error in L↓, for both the IJ and Brunt models.

The large daily range in L↓ results from the large amplitude in daily air temperature. With the small nocturnal fluxes of downward long wave radiation there is a large radiative loss with Q* falling to below -100 W m^{-2} on all nights. The atmospheric transmissivity (the ratio of K↓ at the surface to that at the top of the atmosphere) for the site at solar noon was 0.7 which is identical to that found by Kalma and Badham (1972) for Katherine.

Energy balance

The consistently negligible levels of evaporation and day-to-day consistency in Q* are clearly evident in Table 3 and Fig. 3(c). Leaf stomatal resistance measurements (average over 5–10 sampled leaves) from shrubs adjacent to the site were quite variable, but all exceeded 500 sm^{-1}. Sunlit leaves had values over 1000 sm^{-1}, hence leaf stomata were mostly closed. The plants sampled included those species that were predominant in the main river valley, i.e. mulga and river gums. These large stomatal resistances support the low transpiration rate, although the flux measurements are representative only of below canopy fluxes. Nonetheless the energy used in transpiration and evaporation is very small, especially as there was no early morning dew-fall (see later), so most of the net radiation is partitioned between Q_H and Q_G.

This partitioning varies: average (daily and daytime) soil heat flux increases with time, reaching a maximum on YD 210 – preceding the day showing maximum air and surface temperatures. Average Q_H, on the other hand, decreases from its peak value on YD 205 to a minimum on YD 210 and then increases again through YD 211 and 212. This variable partitioning is directly linked to changes in wind speed (Fig. 3(d)). Low wind speeds lead to greater sensible heat flows into the soil. A maximum (35 per cent) proportion of net radiation flowed into the soil on the day with the lowest mean wind speed (YD 210) and with SW flow. Forty-four per cent of Q* is used in convective heating on YD 205, coinciding with the maximum wind speed, turbulent diffusivities and SE flow.

Unfortunately these ratios do not take into account the lack of closure in the measured energy balance. Some of the residual error term can be attributed to instrument error, but the remainder must arise from advection or heat storage which leads to non-closure beneath the plant canopy. The heat storage term is unlikely to be any larger than 20–30 Wm^{-2} (e.g. McCaughey (1986) found heat storage terms of order 10 per cent of Q* by day and 50 per cent of Q* by night for a mature deciduous forest in Ontario, Canada).

The magnitude of the residual term varies, depending on whether daily or daylight averages are used and whether computed (Q_{G0}) or measured (Q_{G1}) soil heat fluxes are used. Averaged over 24 hours, the residual flux is only 9.8 (using Q_{G1}) or 17 (using Q_{G0}) W m^{-2}, which is 19 per cent and 33 per cent of Q* respectively (Table 3). For the daylight hour averages, the relative sizes of this residual term increase to 23 per cent (Q_{G1}) and 31 per cent (Q_{G0}) of Q*. This residual term can be reduced substantially by acknowledging that Q_H is possibly up to 20 per cent too small (as indicated by the spatial differences in measured heat fluxes, see below). Increasing mean Q_H (daylight hours only) reduces the residual term to 38.7 W m^{-2} (23 per cent of Q*). The frequency distribution of the hourly residual fluxes is depicted in Fig. 4; the most frequent residual flux is in the range -25 to $+25$ W m^{-2}. This small value is biased towards the nocturnal residuals and so is quite large in proportion to the net radiation (around 25 per cent of Q*). The secondary peak of 100–125 W m^{-2} represents the

Table 3. Average energy balance flux densities.

	Average fluxes: Wm^{-2}				*Ratios expressed as a %*				
Key	Q^*	Q_G	Q_H	Q_E	δr	Q_G/Q^*	Q_H/Q^*	Q_G/Q_H	$\delta r/Q^*$
(a) Daily average fluxes (24 hours)									
1	51.8	2.1	34.3	−1.6	17	4	66	6	33
2	51.8	9.3	34.3	−1.6	9.8	18	66	27	19
3	51.8	9.3	40.0	−1.6	4.1[4]	18	77	23	8[4]
(b) Daytime averages ($Q^*>0$)									
1	268.4	78.8	110.5	−3	82.1	29	41	71	31
2	268.4	100.1	110.5	−3	60.8	37	41	91	23
3	268.4	100.1	132.6	−3	38.7[4]	37	49	75	13[4]

Key: 1: using Q_{G0}.
2: using Q_{G1}.
3: increasing Q_H by 20%.
4: residual computed using increased Q_H and Q_{G1}.

residual flux during the day and also represents ca. 25 per cent of the net radiation. Increasing Q_H by 20 per cent would reduce this residual term. The occurrence of the largest residuals at times when the soil heat flux is a smaller component of the energy balance and sensible heat loss is large (viz. YD 211, 212) provides further evidence that Q_H measurements are actually underestimates of the true flux.

Analysis of the diurnal course of the residual term failed to find any link between its magnitude and wind speed, direction or atmospheric stability except for the finding that the term was larger when convective sensible heat flux dominated the daily energy partitioning. Given the less than ideal site, non-closure of the energy balance as expressed in Eqn 1 is to be expected. The residual term is similar in magnitude to other values found in the literture (e.g. Grimmond 1991; Grimmond et al. 1993). This failure to close the energy balance does introduce some uncertainty into our interpretations of the local-scale energy balance, although the general picture should still be valid.

Sensible heat fluxes were measured simultaneously over a 24-hour period at two locations: Q_{H1} are fluxes measured at the main site, Q_{H2} are sensible heat fluxes measured at a height of 2 m at a site 40 m further into the main valley, where the vegetation was more sparse. This comparison (Fig. 5) shows good agreement in trend, but the fluxes at the main site are consistently ca. 20 per cent smaller than those at the open site. If the latter are considered to be 'correct' because the underlying assumptions of the eddy correlation technique are more likely to be met, then Q_{H1} are possibly 20 per cent too small. The mean vertical wind speeds and correlation coefficients at both sites were similar and typical of values at more ideal locations. This 20 per cent difference between Q_{H1} and Q_{H2} illustrates an order of magnitude estimate of the spatial variability in sensible heat flux in this landscape.

Fig. 4 Frequency distribution of residual fluxes.

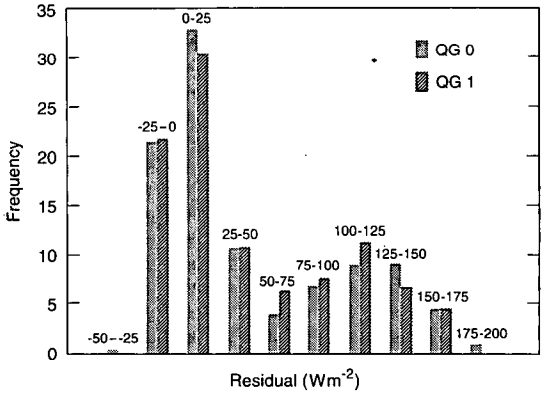

Fig. 5 Spatial intercomparison of measured sensible heat fluxes.

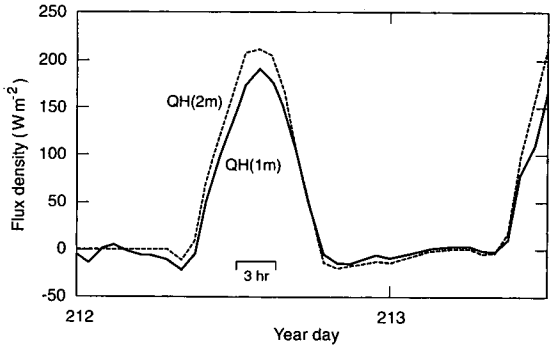

The 'ensemble' (Fig. 6(a)) and two extreme energy budgets (Figs 6(b) and 6(c)) for YD 210 (large Q_G) and YD 205 (where Q_H is the dominant heat flux) illustrate the diurnal path of energy partitioning and some characteristic features of a semi-arid site; early peaking of Q_G (1100 CST, Central Australia Standard Time) and a later peak in Q_H (around 1400 CST). There is a slight asymmetry in the radiative fluxes, a result of a low hill to the NE which delays the increase in radiation and heating in the early morning. All fluxes become positive at around 0900 CST (as do the surface-to-air temperature differences – see below). The transition at sunset to a negative sensible heat flux (i.e. flowing towards the surface) does not coincide with the sign change in Q*. Q_H remains positive until 1900 CST (40–60 mins after Q*) while Q_G turns negative 60–80 mins prior to Q*. Q_G and Q* are in balance when Q_H approaches zero but during the night the radiative loss exceeds the upward flow of heat from the deeper soil layers and is supplemented by a downward-directed sensible heat flow.

These energy balance features are similar to other observations. The sensible heat fluxes are smaller than those presented for a dry lake bed by Sellers (1965). However the ensemble energy balance is remarkably similar to that presented by Grimmond (1991) for a semi-arid landscape in Arizona, USA. The Areyonga energy balances show far less day-to-day variability than those presented in Smith et al. (1994 – northern Queensland) or Wang and Mitsuta (1990 – Gobi Desert) plus Q_H and Q_G fluxes comprise, respectively, a smaller and larger proportion of the net radiation flux than found in these other two studies. Wang and Mitsuta (1990) find significant nocturnal Q_E fluxes, a feature absent in this study.

Fig. 6 Diurnal course of energy balance components; (a) ensemble, i.e. averaged over 10 days of measurements; (b) YD 205, large sensible heat flux; (c) YD 210, large soil heat flux.

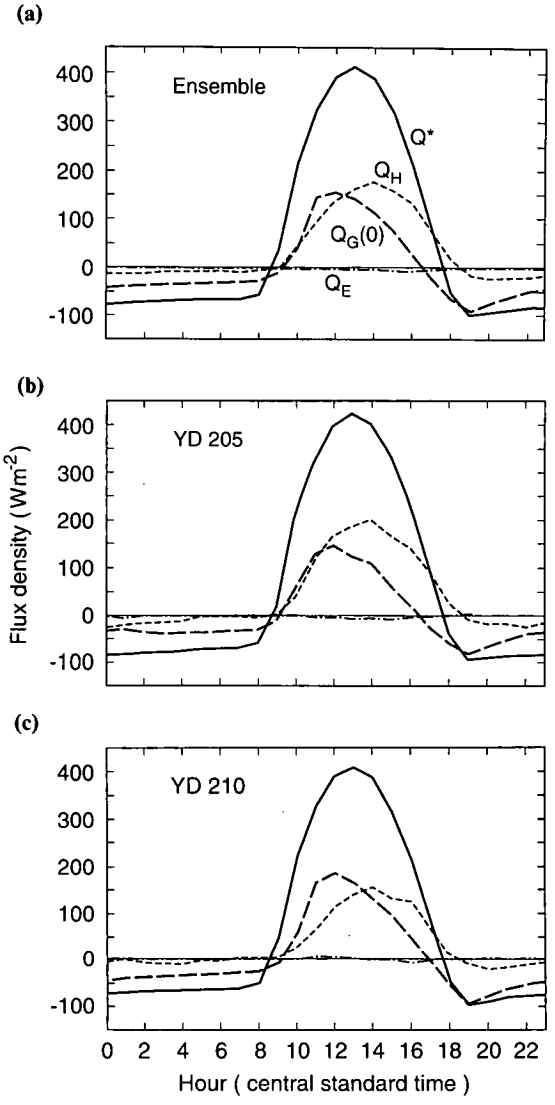

Local-scale climate

Despite the lack of day-to-day variability in the radiation fluxes there is a steady increase in air, surface and soil temperatures (Fig. 7) over the 10-day measurement period. The increasing air temperatures arise from air mass changes as well as changing wind speed and direction and thus energy balance partitioning. The trend in Q_G over the ten measurement days parallels this increase in soil and surface temepratures (recall Fig. 3(c)). The latter peak on YD 211, one day after the peak in Q_G. The increase in aerodynamic resistance (i.e. lower wind speeds) after YD 211 yields lower sensible heat fluxes. This 'sheltering' effect also contributes to the increase over time in T_{air} along with T_s. This overall change in air and surface temperatures has a profound effect on the long wave radiation budget, but little impact on the overall net radiation.

The soil temperatures can be used to compute an approximate damping depth and thermal diffusivity of the soil. This computed diurnal damping depth is a shallow 0.08 m, which translates to a thermal diffusivity of 2.21×10^{-7} $m^2 s^{-1}$, both values are similar to textbook values for dry sand (e.g. Oke 1987).

The surface and air temperatures reveal a consistent, low-level nocturnal radiation inversion, which will be strengthened by cold air ponding in both the tributary and main valleys. The maximum strength of this near-surface inversion is 3.6°C m^{-1}. The transition from a lapse to an

Fig. 7 Time series of hourly: (a) dew-point and air temperatures; (b) soil and air temperatures.

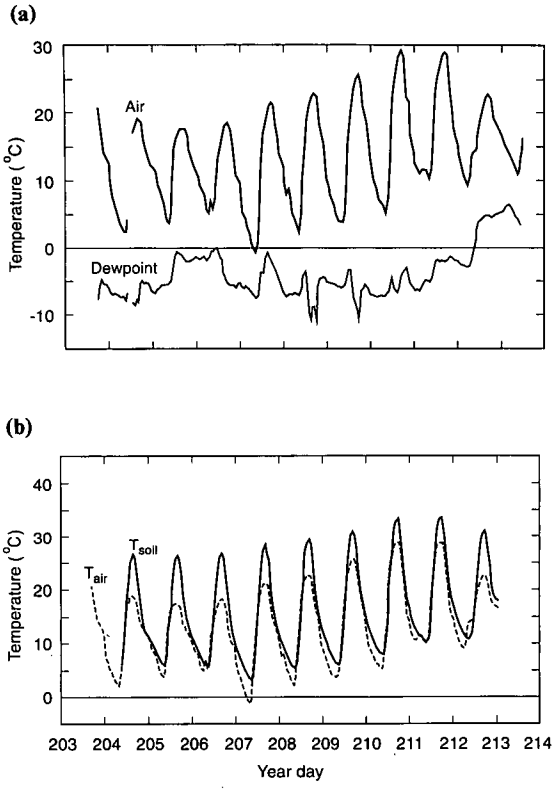

inverted temperature gradient occurs two hours after the air temperature peaks and one hour prior to Q_H turning negative. The change from a negative to a positive sensible heat flow matches the observed change from a nocturnally stable to a diurnally unstable temperature gradient. The time of maximum air temperature (1600 CST) is lagged with respect to T_s (1400 CST) whereas the minimum surface and air temperatures occur almost simultaneously (0600–0700 CST).

The extreme dryness of the location is also revealed in Fig. 7, showing the diurnal variation in dew-point temperatures which are consistently less than air temperatures. Despite overnight surface and air temperatures almost dropping to zero, dew-point was never reached. Certainly, no dew-fall was observed at the site on the instruments or vegetation, although dew on the soil surface would be difficult to observe. The extremely dry atmosphere explains the large nocturnal radiative losses and hence extreme local-scale climate. Interestingly, there is an apparent trend towards increasing atmospheric humidity over time which parallels the increasing temperatures. These coincide with a shift from strong synoptic easterly flow (described as trade wind surges in the July *Monthly Weather Review* published by the Bureau of Meteorology) from 21–25 July (YD 203–207) to lighter N-NW flow after 25 July. The days of maximum (YD 211) and minimum (YD 207) temperatures coincide with the climate statistics presented in the *Monthly Weather Review*, for other locations in central Australia which suggests that the observed microclimate at this site is not atypical of the regional climate.

Conclusions

These measurements quantify the dominant features of the local-scale energy partitioning and hence climate for a site within the desert ranges of semi-arid central Australia. The major influence appears to be the extreme dryness of the atmosphere in the winter months. This results from the feedback between the dominant synoptic regime (northward extension of the subtropical anticyclonic ridge and prevalent easterly trade windflow) with subsiding air, little rainfall and hence no evaporation. This aridity is one of the major controls on the magnitude of the radiative fluxes and subsequent energy partitioning, together with the thermal characteristics of the soil and wind speed. Superimposed on this surface energy partitioning, are variations that arise from changing air-flows which inject air masses with differing thermal and moisture characteristics.

The solar beam is relatively unattenuated (i.e. high atmospheric transmissivity), leading to large inputs of solar radiation. The measured albedo is lower than might be expected and results in a high absorption of solar radiation at the surface. The low thermal diffusivity of the soil and damping depth further concentrates this heating in a relatively shallow layer. The size of the conducted heat flow varies with wind speed. Higher wind speeds lead to large convected sensible heat fluxes but cooler air temperatures. The large degree of surface heating, driven by the radiative input and a fairly shallow heat store means that nocturnal long wave losses are large. Contributing to these large losses is the small downward flux of long wave radiation from a cold and dry atmosphere with a very low emissivity.

These energy and radiation fluxes reinforce the extreme atmospheric aridity and the end result is a climate with extremely low humidity, large solar input and large diurnal range in temperatures (both soil and air). Very little condensation was observed – the dew-point temperature was never reached either by the air or surface temperatures.

However, these data only represent a 10-day interval and there was sufficient evidence that nocturnal dew-fall is possible, especially in the smaller valleys such as inhabited by the Areyonga community. Human habitation may increase the atmospheric humidity and significant cold air ponding may lead to even lower surface and air temperatures. This study was also confined to below canopy fluxes, dew-fall may be more likely to accumulate on the vegetated canopy at night than on the soil surface.

Acknowledgments

We wish to thank John Butcher for his assistance with the field measurements. The permission of the people of Areyonga to establish our monitoring site on their land is gratefully acknowledged. This research was funded from a Macquarie University Research Grant.

References

Brunt, D. 1932. Notes on radiation in the atmosphere. *Agron. J., 62*, 4–8.

Bureau of Meteorology 1992. *Monthly Weather Review*, July and August.

Charney, J., Quirk, W.J., Chow, S.-H. and Kornfield, J. 1977. A comparative study of the effects of albedo change on drought in semi arid regions. *J. Atmos. Sci., 34*, 1366–85.

Cleugh, H.A. and Oke, T.R. 1986. Suburban-rural energy balance comparisons in summer for Vancouver, B.C. *Bound. Lay. Met., 36*, 351–69.

Culf, A.D. and Gash, J.C. 1993. Longwave radiation from clear skies in Niger: A comparison of observations with simple formulas. *Jnl appl. Met., 32*, 539–47.

Duvenani, S. 1964. Dew in Israel and its effect on plants. *Soil Science, 98*, 14–21.

Grimmond, C.S.B. 1992. The suburban energy balance: methodological considerations and results for a mid-latitude west coast city under winter and spring conditions. *Int. J. Climatol., 12*, 481–97.

Grimmond, C.S.B. 1991. Comparisons of measured summer suburban and rural energy balances for a hot, dry city, Tucson, Arizona. *Proceedings of the 10th Conference on Biometeorology and Aerobiology*, Salt Lake City, United States, Amer. Met. Soc.

Grimmond, C.S.B., Oke, T.R. and Cleugh, H.A. 1993. The role of 'rural' in comparisons of observed suburban-rural flux differences. *Proceedings of Joint IAHS-IAMAP Conference*, Yokohama, Japan.

Hacker, J. 1988. The spatial distribution of the vertical energy fluxes over a desert lake area. *Aust. Met. Mag., 36*, 235–43.

Huang, X., Lyons, T.J., Smith, R.C.G., Hacker, J.M. and Schwerdtfeger, P. 1993. Estimation of surface energy balance from radiant surface temperature and NOAA AVHRR sensor reflectances over agricultural and native vegetation. *Jnl appl. Met., 32*, 1441–9.

Idso, S.B. and Jackson, R.D. 1969. Thermal radiation from the atmosphere. *J. geophys. Res., 74*, 5397–403.

Kalanda, B.D., Oke, T.R. and Spittlehouse, D.L. 1980. Suburban energy balance estimates for Vancouver, B.C., using the Bowen ratio-energy balance approach. *Jnl appl. Met., 19*, 791–802.

Kalma, J. and Badham, R. 1972. The radiation balance of a tropical pasture. I. The reflection of short-wave radiation. *Agric. Met., 10*, 251–9.

Kustas, W.B., Goodrich, D.C., Moran, M.S., Amer, S.A., Bach, L.B., Blanford, J.H., Chehbouni, A., Claassen, H., Clements, W.E., Doraiswamy, P.C., Dubois, P., Clarke, T.R., Daughtry, C.S.T., Gellman, D.I., Grant, T.A., Hipps, L.E., Huete, A.R., Humes, K.S., Jackson, T.J., Keefer, T.O., Nichols, W.D., Parry, R., Perry, E.M., Pinker, R.T., Pinter Jr., P.J., Qi, J., Riggs, A.C., Schmugge, T.J., Shutko, A.M., Stannard, D.I., Swiatek, E., van Leeuwen, J.D., van Zyl, J., Vidal, A., Washburne, J. and Weltz, M.A. 1991. An interdisciplinary field study of the energy and water fluxes in the atmosphere-biosphere system over semi-arid rangelands: Description and preliminary results. *Bull. Am. met. Soc., 72*, 1683–1707.

Lyons, T.J., Schwerdtfeger, J.M., Foster, I.J., Smith, R.C.G. and Huang, Xinmei. 1993. Land-atmosphere interaction in a semiarid region: the bunny fence experiement. *Bull. Am. met. Soc., 74*, 1327–34.

McCaughey, J.H. 1986. Energy balance storage terms in a mature mixed forest at Petawawa, Ontarioi — A case study. *Bound. Lay. Met., 31*, 89–101

Oke, T.R. 1987. *Boundary Layer Climates.* Methuen, 2nd Edition, 435 pp.

Ramanathan, V., Cess, R.D., Harrison, E.F., Minnis, P., Barkstrom, B.R., Ahmad, E. and Hartmann, D. 1988. *Science, 247*, 57–63.

Sellers, W.D. 1965. *Physical Climatology.* Chicago Press, 272 pp.

Smith, R.K., Reeder, M.J., Tapper, N.J. and Christie, D.R. 1994. Central Australian cold fronts. *Mon. Weath. Rev.* (in press).

Tapper, N.J. 1988. Surface energy balance studies in Australia's seasonally wet tropics: results from AMEX Phase I and II. *Aust. Met. Mag., 36*, 61–8.

Tapper, N.J. 1991. Evidence for a mesoscale thermal circulation over dry salt lakes. *Palaeogeography, Palaeoclimatology, Palaeoecology, 84*, 259–69.

van Oosterzee, P. 1991. *The Centre: A natural history of Australia's desert regions.* Reed Books, Sydney, Australia, 272 pp.

Wang, J. and Mitsuta, Y. 1990. Evaporation from the desert: Some preliminary results of Heife. *Bound. Lay. Met., 59*, 413–18.